LEO Constellation Design Based on Dual Objective Optimization and Study on PPP Performance

Xin Nie[1(✉)], Min Li[2], Fujian Ma[3], Lei Wang[1,2,3], and Xu Zhang[1,2,3]

[1] China Academy of Space Technology (CAST), Beijing 100094, China
[2] Shandong University, Weihai, China
[3] Wuhan University, Wuhan, China

Abstract. Low-orbit satellites have the advantages of rapid observation geometric changes and strong reception signals. The LEOs play a significant role in accelerating the convergence speed of precise point positioning, and help to provide high-precision positioning services indoors or in areas with severe signal obstruction. However, due to the constraint of the orbit height of low orbit satellites, a larger number of satellites are needed to achieve global coverage compared with medium and high orbit satellites. This paper proposes a LEO constellation design method based on dual-objective optimization, which uses fewer satellites to achieve global coverage. The PPP performance under different boundary conditions is analyzed through simulation. The method proposed in this paper can be widely used in the design of LEO satellite navigation augmentation system, and the research results provide reference and support for the corresponding system demonstration and analysis.

Keywords: LEO · Dual objective optimization · Precise point positioning

1 Introduction

GNSS precision point positioning technology can achieve static centimeter to millimeter level, dynamic decimeter to centimeter level high-precision absolute positioning, but this technology still has two problems [1]. First, that convergence time is too long. To achieve centimeter level or even millimeter level, for single-system positioning, it usually takes 20 min or more to converge. The reconvergence time is almost as long as the first convergence time, which greatly reduces its availability and reliability. Second, The GNSS constellation usually adopts mid-to-high orbit. The satellite signal is attenuated seriously during the propagation process, resulting in weak signal strength on the ground, which is not conducive to positioning services indoors or in cities, canyons, forests and other areas with severe signal obscuration. Anti-jam performance is difficult to guarantee. Low-orbit satellites have the advantages of rapid observation geometric changes and strong ground reception signals. They play a significant role in accelerating the convergence speed of precise point positioning, and help to provide high-precision positioning services indoors or in areas with severe signal obscuration [2, 3]. Compared

C. Yang and J. Xie (Eds.): *China Satellite Navigation Conference (CSNC 2021) Proceedings*, LNEE 773, pp. 197–207, 2021.
https://doi.org/10.1007/978-981-16-3142-9_18

with medium and high orbit satellites, due to the constraint of the orbit height of low orbit satellites, a larger number of satellites are needed to achieve global coverage.

This paper proposes a LEO constellation design method based on dual-objective optimization which uses coverage performance and the number of satellites as optimization goals, to achieve global coverage performance and uses with fewer satellites. Based on the design of the constellation scheme and the measured data, the PPP performance based on the LEO constellation under different boundary conditions is analyzed through simulation. The method proposed in this paper can be widely used in the design of LEO satellite navigation enhancement system, and the research results provide reference and support for the corresponding system demonstration and analysis.

1.1 LEO Satellite Features

LEO satellites generally have an orbit height of 400 km to 1500 km. Compared with the medium and high orbits used by GPS and Beidou GNSS systems, they have the following characteristics:

(1) The track is low, the signal attenuation is small, and the received signal strength is high, which is conducive to positioning in a sheltered environment and indoors. Since LEO satellites have a lower orbit than MEO satellites, the signal fading is small. According to the calculation of the LEO satellite orbit height of 1100 km and the MEO satellite orbit height of 21528 km, considering the use of a single beam antenna, the antenna beam angle of the LEO is is twice the angle of the MEO.

$$k = \frac{\arcsin(\mathrm{R/R + H}_{LEO})}{\arcsin(\mathrm{R/R + H}_{MEO})} = \frac{\arcsin(35786/36886)}{\arcsin 35786/57786} \approx 2,$$

where R is the radius of the earth, $\mathrm{H_{LEO}}$ and are the height of LEO and LEO, respectively. According to the formula of the relationship between antenna aperture and half-beam angle $D = 70\,\lambda/\theta_{1/2}$, if the aperture of a single-beam antenna is 1/2, the antenna gain will decrease by 6 dB. In summary, when the single-beam antenna is used, the satellite transmitting power is the same, and the power reaches the ground is enhanced by 20 dB (Fig. 1).

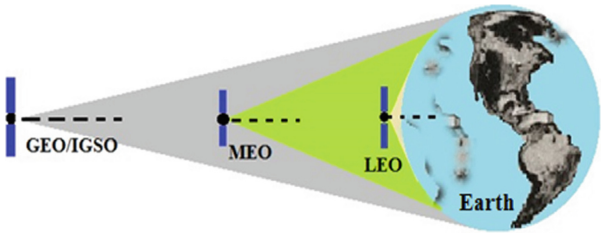

Fig. 1. Schematic diagram of satellite distance and coverage of different orbital altitudes

(2) The orbit is low and the coverage area of a single satellite is small. According to calculations, 7 LEO satellites are required to cover the visible range of 1 MEO satellite [4], and a larger number of satellites are required to achieve the same coverage effect.
(3) The observation geometry changes quickly, which is conducive to rapid convergence. As shown in Fig. 2, LEO running for 31 s is equivalent to the geometrical change degree of GPS running for 20 min. In the same time period, the LEO trajectory is longer, the geometry changes quickly, and the convergence time during PPP positioning will be greatly shortened.
(4) The perturbation force is complicated, and the precise orbit determination and prediction are difficult. During the operation of LEO satellites, the dynamic orbit determination model is more complicated under the influence of various forces such as the earth's gravity field, ocean tide, solid tide, sunlight pressure, and atmospheric resistance.

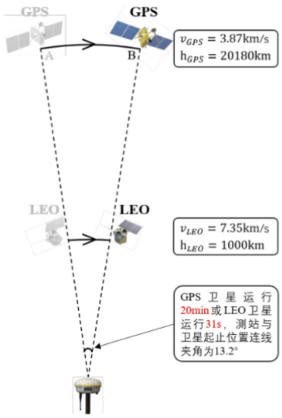

Fig. 2. Comparison of LEO and MEO satellite observation geometry

1.2 Analysis of the Influence of Atmospheric Drag on the Number of Low-Orbit Satellites

Taking into account the 31 × 31-order earth gravity field model, ocean tide, solid tide, sunlight pressure, Jacchia 1970 atmospheric drag model and three-body gravity [5], the satellite surface-to-mass ratio is 0.01 m^2/kg, and the orbit height of satellite is between 500 km and 1100 km, the impact was carried out. The analysis results are shown in Table 1. It can be seen that the atmospheric resistance mainly has a significant influence on the orbital semi-major axis between 500 km and 800 km, so the proposed low-orbit satellite constellation orbit height is between 900 km and 1500 km.

Table 1. The influence of atmospheric drag on the six elements of the orbit

Orbit height (km)	Semi-major axis (m)	Eccentricity	Inclination	RAAN	Perigee angular distance	Mean anomaly
500	8131.5	6.09e−04	0.0162	0.0639	9.1467	359.9227
600	951.5	8.18e−05	0.0018	0.0071	3.0328	359.7060
700	497.98	4.56e−05	9.05e−04	0.0037	1.5349	359.6837
800	157.03	1.37e−05	2.74e−04	0.0011	2.2769	10.8145
900	31.91	2.52e−06	5.51e−05	2.18e−04	−0.1777	3.9658
1000	32.66	1.73e−06	5.43e−05	2.18e−04	−0.2131	2.4606
1100	15.64	1.49e−06	−3.78e−05	1.14e−04	0.0470	−0.0169

1.3 Optimal Design of Low-Orbit Navigation Constellation Based on Dual Objective Optimization

The adopted constellation configuration is Walker constellation, expressed as N/P/F, where N is the total number of satellites, P is the number of orbital planes, and F is the phase factor. The low-orbit satellites that make up the global navigation constellation should meet two primary conditions: GDOP should be as small as possible to meet user navigation accuracy requirements, and the number of satellites should be as small as possible to reduce system construction costs. Therefore, two objective functions are set:

$$\begin{cases} Fitness_1 = \max\limits_{t\in(0,T_P)} \max\limits_{F\in(0,P-1)} \max\limits_{r_{P\in Earth}} GDOP\left(r_p, t, c\right) \\ Fitness_2 = s \times p \end{cases} \tag{1.1}$$

Dividing the world into a grid of 6° × 6°, the largest GDOP value among all grid points in the P satellite configurations during the satellite orbit period T is Fitness1, Fitness2 is the number of satellites. Use parallel NSGA-III algorithm [6, 7] for optimization search.

1.3.1 Single Walker Constellation Design

The global average number of visible satellites is 4, 5, and 6, and the number of visible satellites varies with latitude when the orbit height is 900 km. It can be seen that the number of visible satellites in the world under a single Walker constellation is unevenly distributed.

1.3.2 Compound Walker Constellation Design

Due to the uneven global distribution of a single Walker constellation, a hybrid Walker constellation composed of orbital heights of 900 km and 1200 km is designed, and the parallel NSGA-III algorithm is used to search. When the average number of visible satellites is 4, 5, and 6, the results are shown in Table 2.

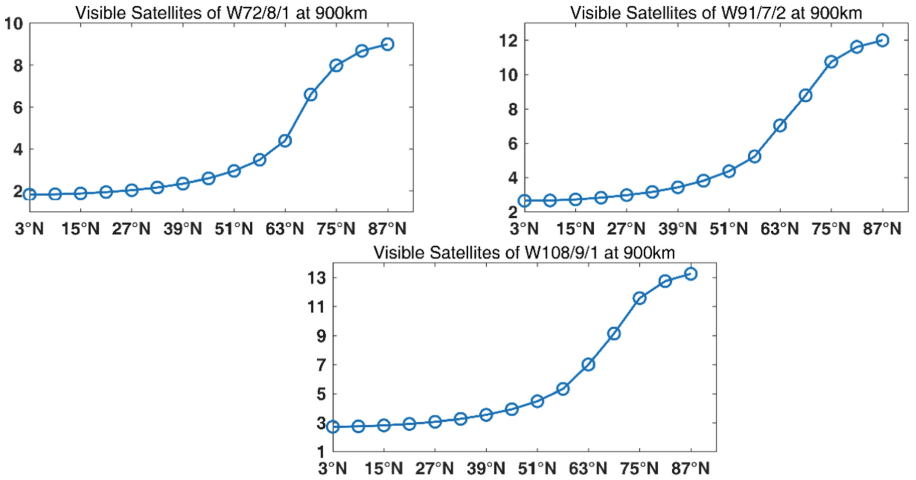

Fig. 3. The number of satellites varies with latitude

Table 2. Composite constellations corresponding to different visible satellite numbers

Average visible satellites	Orbital height (km)	Constellation configuration	Orbital inclination (deg)
4	900	W56/8/4	42.85
	1200	W32/8/2	87.59
5	900	W81/9/1	36.42
	1200	W40/10/1	85.0
6	900	W64/8/4	37.85
	1200	W60/10/4	87.85

The number of visible satellites in each hybrid constellation varies with latitude as shown in Fig. 4. It can be seen that the compound Walker constellation composed of two orbital heights can achieve a more uniform global distribution (Fig. 5 and 6).

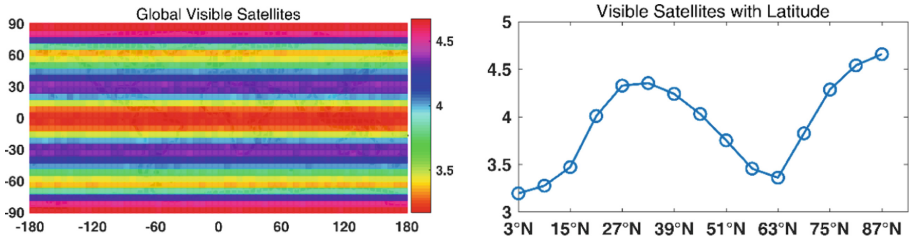

Fig. 4. The number of visible satellites in 4 mixed constellations of average visible stars varies with latitude

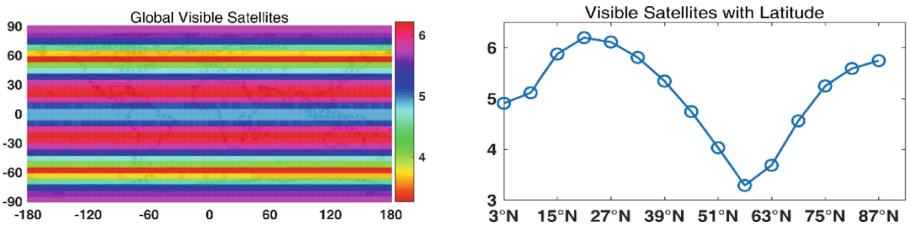

Fig. 5. The number of visible satellites in 5 mixed constellations of average visible stars varies with latitude

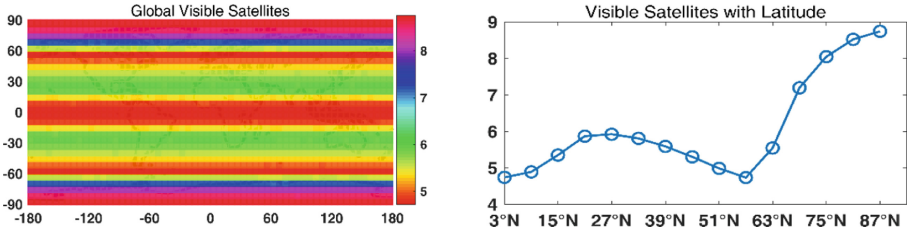

Fig. 6. The number of visible satellites in 6 mixed constellations of average visible stars varies with latitude

1.4 Research on the Performance of Low-Orbit/GNSS Multi-system PPP

1.4.1 LEO/GNSS Multi-system Fusion Positioning Model

The theoretical method and mathematical model of LEO/GNSS fusion positioning: The real-time orbit and clock error information of LEO satellites can be obtained through the precise orbit determination of LEO satellites. Assuming that the station receiver tracks the satellite, the original basic observation equations of LEO/GNSS pseudorange and carrier phase can be expressed as:

$$\begin{aligned} p_{r,j}^{s} &= \mu_r^s \Delta x_r + t_r - t^s + d_{r,j}^{s} - d_j^s + \beta_{r,j}^{s} I_{z,r} + m_r^s Z_r + \varepsilon_{r,j}^{s} \\ l_{r,j}^{s} &= \mu_r^s \Delta x_r + t_r - t^s - \beta_{r,j}^{s} I_{z,r} + m_r^s Z_r + \lambda_j^s \left(N_{r,j}^{s} + b_{r,j}^{s} - b_j^s \right) + \xi_{r,j}^{s}, \end{aligned} \tag{1.2}$$

where $p_{r,j}^{s}$ and $l_{r,j}^{s}$ is the observed value minus calculated value (OMC) of the pseudorange and carrier phase observations, in meters; j is the frequency number; μ_r^s is the linearized receiver-to-satellite unit line vector, Δx_r is the receiver column vector of coordinate increments relative to the prior position, t_r and t^s are the clock difference between the receiver and the satellite respectively, d_j^s and $d_{r,j}^{s}$ are the frequency-dependent UCD on the receiver and the satellite respectively, and $I_{z,r}$ is the total zenith ionospheric delay. $\beta_{r,j}^{s} = \gamma_r^s \cdot 40.3 \Big/ f_j^2$ is the frequency-dependent factor, where γ_r^s Is the ionospheric projection function, f_j is the corresponding frequency, Z_r is the tropospheric zenith delay, m_r^s is the corresponding projection function, $N_{r,j}^{s}$ is the integer ambiguity, λ_j^s is the

corresponding wavelength, $b_{r,j}^{s}$ and b_{j}^{s} is the frequency-dependent UPD on the receiver and satellite respectively, and $\varepsilon_{r,j}^{s}$ are $\xi_{r,j}^{s}$ the measurement noise of the pseudorange and carrier phase observations.

In addition, due to different signal frequencies and signal structures, multi-system GNSS combined PPP should consider IFB. Taking the GPS system as the reference system, the ionospheric combined observation equation of the four-system combined PPP can be expressed as

$$\begin{aligned} p_{r,IF}^{s,G} &= \mu_{r}^{s,G}\Delta x_r + \bar{t}_r + m_{r}^{s,G}Z_r + \varepsilon_{r,IF}^{s,G} \\ l_{r,IF}^{s,G} &= \mu_{r}^{s,G}\Delta x_r + \bar{t}_r + \overline{N}_{r,IF}^{s,G} + m_{r}^{s,G}Z_r + \xi_{r,IF}^{s,G} \end{aligned} \tag{1.3}$$

$$\begin{aligned} p_{r,IF}^{s,i} &= \mu_{r}^{s,i}\Delta x_r + \bar{t}_r + IFB_{r}^{s,i-G} + m_{r}^{s,i}Z_r + \varepsilon_{r,IF}^{s,i} \\ l_{r,IF}^{s,i} &= \mu_{r}^{s,i}\Delta x_r + \bar{t}_r + IFB_{r}^{s,i-G} + \overline{N}_{r,IF}^{s,i} + m_{r}^{s,i}Z_r + \xi_{r,IF}^{s,i} \end{aligned} \tag{1.4}$$

In the formula, G represents GPS, $i \in \{R, C, E, L\}$ respectively represents GLONASS, BDS, Galileo system and low-orbit satellite; the receiver clock error parameter can be expressed as

$$\bar{t}_r = t_r^G + d_{r,IF}^G \tag{1.5}$$

At the same time, the IFB parameters and ISB parameters are respectively

$$IFB_{r}^{s,i-G} = d_{r,IF}^{s,i} - d_{r,IF}^{G} \tag{1.6}$$

In the formula, the ionospheric-free combined floating-point ambiguity $\overline{N}_{r,IF}^{s,G}$, and $\overline{N}_{r,IF}^{s,i}$ includes the ionospheric-free combined UPD at the receiver end and the satellite end; $d_{r,IF}^{s,i}$ and $d_{r,IF}^{G}$ are the ionospheric-free combined UCD at the satellite end. The ambiguity can then be expressed

$$\begin{aligned} \overline{N}_{r,IF}^{s,G} &= N_{r,IF}^{s,G} - d_{r,IF}^{G} - d_{IF}^{s,G} \\ \overline{N}_{r,IF}^{s,i} &= N_{r,IF}^{s,i} - IFB_{r}^{s,i-G} - d_{IF}^{s,i} \end{aligned} \tag{1.7}$$

Suppose that the receiver observes satellites, where n_G, n_R, n_E, n_C, n_L are the numbers of GPS, GLONASS, BDS, Galileo and LEO satellites, respectively. Let the weight matrix of the observation value be P, the observation equation of the low-orbit satellite/GNSS combined PPP can be expressed as

$$L = AX + e \tag{1.8}$$

where is L the OMC vector, A is the design matrix, X is the parameter vector, and e is the measurement noise vector. Assuming that $\overline{N}$ and $\overline{W}$ are the normal equation information after the adjustment of the previous epoch, the PPP parameter estimation result of the combination of low-orbit satellite and GNSS can be expressed as

$$\begin{aligned} \hat{X} &= \left(A^T PA + \overline{N}\right)^{-1}\left(A^T PL + \overline{W}\right) = N^{-1}W \\ V &= A\hat{X} - L \\ \hat{\sigma}_0 &= \sqrt{\frac{V^T PV}{n-t}} \end{aligned} \tag{1.9}$$

In the formula, N and W is the normal equation after contributing the observation information of this epoch, V is the residual vector of dimension, $\hat{X}$ is the parameter vector of dimension, and $\hat{\sigma}_0$ is the unit weight STD.

1.4.2 GNSS/LEOConstellation Simulation

GNSS includes GPS, GLONASS, Galileo and BDS-3 systems. There are 30 satellites in the BDS-3 full constellation, including 3 geostationary orbit satellites (GEO), 3 inclined geostationary orbit satellites (IGSO) and 24 medium orbit (MEO) satellites [8]. GPS, GLONASS, and Galileo satellites are consistent with the officially announced constellation configuration. The constellation of the LEO satellite is configured as a polar-earth orbit satellite. Two configurations are set up here, namely the Walker (96/8/1) constellation and the Walker (64/8/4) + Walker (60/10/4) composite constellation.

1.4.3 Simulation of Observation Data

In order to evaluate the LEO constellation to augument the BD-3 PPP positioning performance, the MGEX station IFNC, which can observe BD-3 satellites in China, is used with a sampling interval of 1s and a sampling duration of 5h. The observation information is as follows: GPS satellites are L1 (1575.42 MHz) and L5 (1176.45 MHz) dual-frequency observation data; the observation frequencies of BDS-3 are B1C (1575.42 MHz) and B2a (1176.45 MHz), LEO uses dual-frequency observation data of B1C and B2a. The observation data simulation fully considers various error sources. First, the observable angular distances of different types of satellites are carefully calculated and distinguished, and the carrier phase and code pseudorange observation noise are optimized. The dry component of the tropospheric delay is calculated by the Saastamoinen model, the wet component is estimated by the actual PPP, and the mapping function is GMF. The receiver clock error and the inter-system error parameter ISB adopts the estimated value of the measured data as the analog value input. Both the satellite clock error and the receiver clock error use MGEX clock error products. Each ambiguity of each satellite consists of a constant integer deviation and a decimal floating-point value. The code pseudorange and carrier phase noise are set to 0.1 m and 5 mm, respectively. In addition, phase entanglement, relativistic effects and solid tide corrections are accurately calculated by known models.

1.4.4 Simulation Analysis

In order to analyze the LEO-enhanced GNSS positioning effect in the “urban canyon” environment, the PPP performance of GPS/GLONASS/Galileo/BD-3/LEO (GRECL)

under signal occlusion was simulated and analyzed. In terms of signal occlusion simulation, considering the urban high-rise environment, the signal may be intermittent when the carrier is in motion. Therefore, cut-off height angles of 10, 20, 30, and 40° are set. The process of re-convergence of the precision point positioning service after signal interruption was considered in the simulation process. The occlusion is 1 min each time, with an interval of 15 min. The combined positioning result of 96 LEO low-orbit satellite and GREC system is shown in Fig. 7. When the RMS of the three-dimensional PPP result is better than 0.1 m, the positioning result is considered convergent.

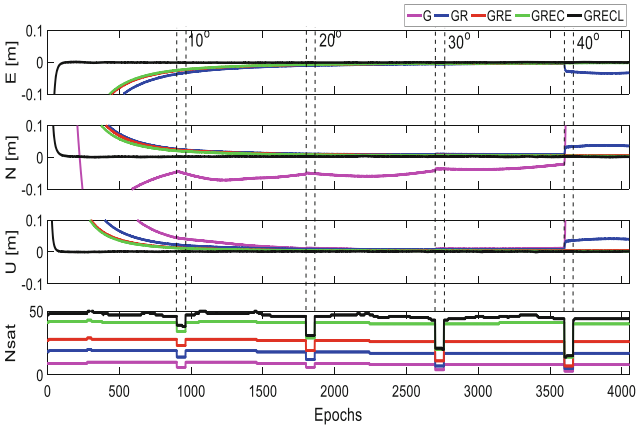

Fig. 7. Different GPS/BDS/LEO positioning results with cut-off angles of 10 to 40°

(1) The convergence time of single GPS (G), GPS/BDS (GC) combination, GPS/LEO (GL) combination, GPS/BDS/LEO (GCL) combination system is 20.6, 16.2, 4.2, and 4.0 min, respectively. An observation station JFNG (Jiufen, Shanxi, China) in a mid-latitude area can observe an average of 3–4 LEO satellites, which can shorten the convergence time to less than 5 min, which is 75.3% shorter than the GC convergence time.

(2) The positioning accuracy of single GPS is basically 5–10 cm within the first 1 h, which is significantly lower than the GC, GL and GCL solutions. When the height cut-off angle is 10, 20, and 30°, the results of each type of solution are basically not affected. Especially for the GL solution, about 11 satellites can be observed without lowering the altitude angle. When the cut-off angle reaches 30°, although the number of satellites observed is the same as GPS (only 5), due to the adopted sequence inertia adjustment, the accuracy is Can still maintain the previous level. When the cut-off angle is 40°, the number of GPS and GL observable satellites drops to 3, and PPP can no longer be achieved. The GC and GCL results are basically not affected, mainly because the number of observable satellites can still be maintained at about 10.

Figure 8 shows the positioning results of Walker (64/8/4) + Walker (60/10/4) low-orbit satellites and GREC at different observation elevation angles. The positioning convergence time of GREC is about 9 min. Due to the increase in the number of LEO satellites, the positioning time of GRECL is shortened to 1–2 min.

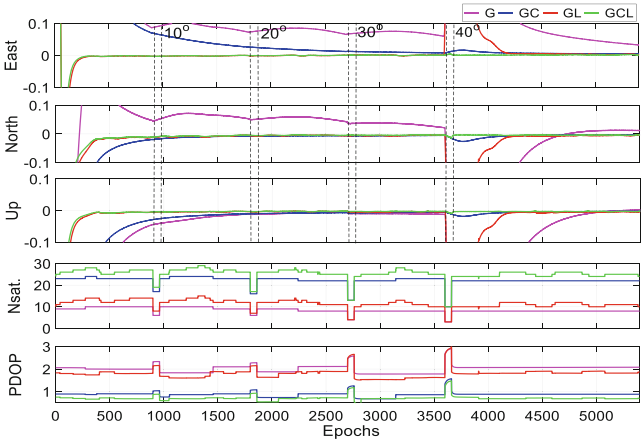

Fig. 8. Different GPS/BDS/LEO positioning results with cut-off angles of 10 to 40°

1.5 Conclusion

Compared with medium and high orbit satellites, due to the constraint of the orbit height of low orbit satellites, a larger number of satellites are needed to achieve global coverage. This paper proposes a LEO constellation design method based on dual-objective optimization which uses coverage performance and the number of satellites as optimization goals to achieve global coverage performance with fewer satellites. Based on the design of the constellation scheme and measured data, the PPP performance based on the LEO constellation under different boundary conditions is analyzed through simulation, including the PPP performance under different constellation configurations, multi-system combinations, and typical use scenarios is given. Single GPS (G), GPS/BDS (GC) combination, the convergence time is 20.6, 16.2 min, respectively, GREC positioning convergence time is about 9 min. With LEO participates in positioning, the convergence time is greatly shortened. 96 LEO satellites can shorten the convergence time to less than 5 min, which is 75.3% shorter than the GC convergence time. When the number of satellites increases to about 120, the GRECL positioning time is shortened to 1 min. At the same time, for high observing cut-off angles, multiple systems will help improve the continuity and availability of positioning services. The method proposed in this paper can be widely used in the design of LEO satellite navigation enhancement system, and the research results provide reference and support for the corresponding system demonstration and analysis.

References

1. Li, X., Li, X., Liu, G., et al.: Triple-frequency PPP ambiguity resolution with multi-constellation GNSS: BDS and Galileo. J. Geod. **93**, 1105–1122 (2019).https://doi.org/10.1007/s00190-019-01229-x
2. Lawrence, D., Cobb, S., Gutt, G.: Navigation from LEO: Current capability and future promise, GPS world [OL]. http://gpsworld.com/ navigation-from-leo-current-capability-and-future-promise/,2019
3. Fischer, J.: STL - Satellite Time and Location [OL]. https://www.orolia.com/sites/default/files/document-files/STL-MaritimeApplicationsV4.pdf (2017)
4. Reid, T.: Orbital Diversity For Global Navigation Satellite Systems. Stanford University (2017)
5. Montenbruck, O., Gill, E., Kroes, R., et al.: Rapid orbit determination of LEO satellites using IGS clock and ephemeris products. GPS Solution **9**, 226–235 (2005)
6. Deb, K., Pratap, A., Agarwal, S., Meyarivan, T.: A fast and elitist multiobjective genetic algorithm: nsga-II. IEEE Trans. Evol. Comput. **6**(2), 182–197 (2002)
7. Deb, K., Jain, H.: An evolutionary many-objective optimization algorithm using reference-point-based nondominated sorting approach, part I. IEEE Trans. Evol. Comput. **18**(4), 577–601 (2014)
8. China Satellite Navigation Office, Development of the BeiDou Navigation Satellite System(Version 4.0) [OL] (2019). http://www.beidou.gov.cn/xt /gfxz/201912/P020191227430565455478.pdf